Available online at www.sciencedirect.com
SCIENCE DIRECT
Journal of Molecular Catalysis A: Chemical 239 (2005) 144–150
JOURNAL OF MOLECULAR CATALYSIS A: CHEMICAL
www.elsevier.com/locate/molcata

# Effects of synthesis parameters on the physico-chemical and photoactivity properties of titania–silica mixed oxide prepared via basic hydrolyzation

Qiujing Yang [a], Chao Xie [a], Zili Xu [a,*], Zhongmin Gao [b], Ziheng Li [c], Dejun Wang [c], Yaoguo Du [a]

[a] College of Environment and Resources, Jilin University, Changchun 130023, China
[b] College of Chemistry, State Key Laboratory of Inorganic Synthesis and Preparative Chemistry, Jilin University, Changchun 130023, China
[c] College of Chemistry, Jilin University, Changchun 130023, China

Received 13 April 2005; received in revised form 3 June 2005; accepted 5 June 2005
Available online 18 July 2005

**Abstract**

Titania–silica mixed oxide ($TiO_2$–$SiO_2$) was prepared from the alkoxides: titanium tetrabutoxide (TBOT) and tetraethyl orthosilicate (TEOS), by using an ammonia–water solution as the hydrolysis catalyst. Variables included synthesis route, aging time, the type of alcohol, and calcination temperature. The materials were then evaluated as photocatalysts for the decomposition of *n*-heptane. Experimental results revealed: (1) the photoactivity of $TiO_2$–$SiO_2$ prepared via the route that Ti sol and Si sol were simultaneously and slowly added, was significantly enhanced due to its good homogeneity. However, for pure $TiO_2$ the route that Ti sol was slowly added into ammonia–water solution was effective in inhibiting the growth of crystalline size and therefore improving the photoactivity; (2) longer aging time promoted the hydrolysis of TEOS. As a result, the intimate interaction between titania and silica (Ti–O–Si hetero linkages) were strengthened and the photoactivity was increased; (3) $TiO_2$–$SiO_2$ prepared by using ethanol as the solvent had the best combination of crystalline size, crystallinity, and homogeneity, thus, it exhibited the best photoactivity among the mixed oxides prepared via different alcohols; (4) 600 °C calcined $TiO_2$–$SiO_2$ possessed excellent photoactivity as compared with that calcined at 400 or 800 °C due to the good crystallinity and the synergism between Ti–O–Si hetero linkages and surface hydroxyl groups.


*Keywords:* Titania–silica mixed oxide; Basic hydrolyzation; Synthesis parameters; Homogeneity; Photoactivity

## 1. Introduction

$TiO_2$–$SiO_2$ represents a promising class of photocatalysts due to its possible applications in environment cleanup [1]. For practical application of $TiO_2$–$SiO_2$, further enhancing its photocatalysis efficiency is necessary. It has been widely recognized the photodegradation behavior of catalyst is closely correlated to its physico-chemical properties such as crystalline size, surface area and crystallinity, which are greatly influenced by the various synthesis parameters [2–15]. Therefore, recently some efforts were devoted to investigating the influences of various synthesis parameters on $TiO_2$–$SiO_2$. For example, Xu et al. studied the photoactivity of $TiO_2$ loaded on silica powders by using $TiO_2$ sol prepared via hydrolyzing titanium tetrabutoxide in an acid environment [8]. Furthermore, Baiker and co-workers systematically investigated the effects of a series of preparation parameters on the structure and chemical properties of $TiO_2$–$SiO_2$ prepared by using acid as hydrolysis catalyst [9–11].

We can see some studies concerning the structure, surface and photoactivity properties of $TiO_2$–$SiO_2$ prepared via various synthesis parameters have been carried out, however, most of them used acid as the hydrolysis catalyst. Recently, we noted an interesting study reported by Yu et al. that the phase structure, texture and photoactivity of titania are strongly altered by the presence of acidic or basic hydrolysis catalyst [16]. They found when $HNO_3$ is used, the crystallization of anatase phase and growth of brookite phase are enhanced. In contrast, $NH_4OH$ not only retards the phase

* Corresponding author.
*E-mail address:* xuzl@jlu.edu.cn (Z. Xu).

1381-1169/$ – see front matter © 2005 Published by Elsevier B.V.
doi:10.1016/j.molcata.2005.06.004

transformation of titania, but also suppresses the growth of brookite phase. Additionally, it was reported monodispersed silica spherical particles could be obtained by hydrolysis of TEOS in ammonia–water solution [17]. Yu and co-workers [18] carefully checked the formation mechanism of monodispersed silica particles under different reaction conditions, and discovered the presence of ammonia–water greatly influences the crystalline size of primary silica particles. Clearly, the ammonia–water solution simultaneously has a remarkable influence on the formation of primary titania and silica particles. Hence, we deduce using ammonia–water as the hydrolysis catalyst to synthesize $TiO_2$–$SiO_2$ should have a deep influence on its final physico-chemical and photoactivity properties. But, none of study in this aspect is reported. So, it should be a meaningful work to investigate the influences of various synthesis parameters on the physico-chemical and photoactivity properties of $TiO_2$–$SiO_2$ prepared by using ammonia–water as the hydrolysis catalyst.

## 2. Experimental

### 2.1. Preparation of catalysts

All chemicals in this study were used as received without any further purification. TBOT (≥98%) and TEOS (≥98%) were selected as the source of titania and silica, respectively. Here, we give a typical procedure for preparing $TiO_2$–$SiO_2$ containing 16.6 mol.% silica. Firstly, 17.0 ml TBOT was mixed with 5.1 ml acetylacetone and 10.0 ml anhydrous alcohol. Then, 2.25 ml TEOS was mixed with the solution containing 10.8 ml bidistilled water, 23.9 ml ammonia–water ($NH_3$, 28%) and 20.0 ml anhydrous alcohol under stirring. The final step was to mix the sols of Ti and Si via two different synthesis routes.

Route A: Ti sol was slowly added into Si sol under stirring.
Route B: Ti and Si sols were simultaneously and slowly added into the beaker containing 10.0 ml alcohol under stirring.

After all the above operations were done, the samples were aged in the beaker covered by plastic film for 24 or 72 h. $TiO_2$–$SiO_2$ with different silica contents were obtained by only varying the dosage of TEOS. Pure $TiO_2$ was prepared by the same procedure illustrated above, except no TEOS was added. Finally, the samples obtained were evaporated and dried under infrared lamp, followed by calcination at the certain temperature for 2 h in air, and then ground into fine powders.

In this paper, pure $TiO_2$ and $TiO_2$–$SiO_2$ were labeled as $TiO_2$–R–*H*–*T* and $TiO_2$–*X*$SiO_2$–R–*H*–*T* (*X*: mol.% of silica in the mixed oxide, R: the synthesis route, *H*: the aging time, *T*: the calcination temperature), respectively. If not pointed out, the alcohol used was ethanol.

### 2.2. Catalyst characterization

The crystalline phases of samples were characterized by a Bruker D8 GADDS X-ray diffractometer using Cu Kα radiation (λ = 1.54056 Å). In addition, the crystalline size *D* was estimated from the width of lines in the X-ray pattern with the aid of the Scherrer formula: $D = K\lambda/(\beta \cos\theta)$, where λ is the wavelength of the X-ray used, $\beta$ is the width of the line at the half-maximum intensity, and K is a constant. FT-IR spectra for the samples were obtained by utilizing a Nicolet Impact 410 Fourier transform infrared spectrophotometer. Surface photovoltage spectroscopy (SPS) were obtained with the surface photovoltage spectrometer that has been described elsewhere [19]. X-ray photoelectron spectroscopy (XPS) measurements were performed in a VG ESCALAB MKΠ X-ray photoelectron spectrometer. The X-ray source emitted Mg Kα radiation (1253.6 eV). For all the binding energy obtained, the pressure was maintained at $6.3 \times 10^{-7}$ Pa. Binding energies were calibrated with respect to the signal for adventitious carbon (binding energy = 284.6 eV).

### 2.3. Photocatalytic activity tests

The photocatalytic activity experiments were carried out at room temperature using a 300 ml quartz reactor (4.4 cm i.d. and 20 cm length). In the experiment, 0.1 g catalyst was spread uniformly over the internal surface of the reactor. After this, the reactor was evacuated and then filled with *n*-heptane (0.1% v/v), oxygen (20% v/v), and balance nitrogen to a total pressure of 1 atm. The reaction was started by turning on a 400 W high-pressure mercury lamp. The primary wavelength distribution of this lamp is at 365 nm and the light intensity is 5.3 mW $cm^{-2}$ at 15 cm away from the lamp. The concentration of reactant in the reactor was measured with a Hewlett–Packard 4890D gas chromatograph equipped with a flame ionization detector (FID).

In this paper, the conversion rate towards *n*-heptane was calculated by $(C_0 - C)/C_0$, where *C* is the concentration of *n*-heptane after irradiation as a function of reaction time and $C_0$ is the concentration of *n*-heptane after adsorption equilibrium and before the irradiation in the presence of catalyst. The adsorption percentage towards *n*-heptane was obtained by $(C_1 - C_0)/C_1$, where $C_1$ is the concentration of *n*-heptane without catalyst and illumination and $C_0$ is the same as that mentioned above.

## 3. Results and discussion

### 3.1. Effects of synthesis route and aging time on the structure and photoactivity of catalysts

The photoactivities of pure $TiO_2$ and $TiO_2$-16.6% $SiO_2$ prepared via different routes and aging time were shown in Fig. 1. The $\ln(C_0/C)$ value, where $C_0$ and $C$ are identical to those described previously, increases linearly with the

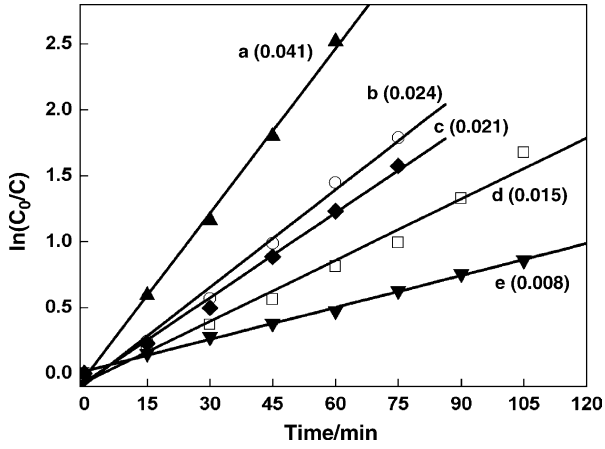


Fig. 1. Photodegradation kinetics of *n*-heptane by the catalysts prepared via different synthesis routes and aging time, the number in the parenthesis is reaction rate constant: (a) $TiO_2$-16.6% $SiO_2$–B–72–600; (b) $TiO_2$-A–72–600; (c) $TiO_2$-16.6% $SiO_2$–B–24–600; (d) $TiO_2$-16.6% $SiO_2$–A–72–600; (e) $TiO_2$–B–72–600.

irradiation time, indicating the photocatalytic reactions follow a first-order rate law. The first-order rate constants listed in the parenthesis of Fig. 1 are useful to compare the relative activities of various catalysts. For $TiO_2$–A–72–600, since it was prepared by directly adding Ti sol into ammonia–water solution, the ratio of $OH^-$/Ti in the reaction solution is much higher in contrast to that of $TiO_2$–B–72–600 prepared by simultaneously and slowly adding Ti sol and ammonia–water solution. Thus, more $OH^-$ ions are adsorbed on the primary titania particles of $TiO_2$–A–72–600 to repel those particles to form a stable sol with a minimum degree of aggregation. Therefore, upon calcination, $TiO_2$–A–72–600 has smaller crystalline size, as shown in Table 1, and better photoactivity in contrast to $TiO_2$–B–72–600.

Similar to $TiO_2$–A–72–600, $TiO_2$-16.6% $SiO_2$–A–72–600 should have more $OH^-$ ions on its primary titania particles than those of $TiO_2$-16.6% $SiO_2$–B–72–600. Although higher concentration of identical charges on primary titania particles can effectively retard the aggregation, unfortunately, it will also prevent the intimate interaction between titania and silica. Therefore, in $TiO_2$-16.6% $SiO_2$–A–72–600 more silica will exist as an independent form without intimate interaction with titania. In terms of the previous studies [4–6], the addition of silica into titania has two effects on the photocatalysis behavior of titania. One is to enhance its photoactivity through the formation of Ti–O–Si hetero linkages, and the other is a side effect because silica is inactive in the photocatalysis process. So, it can be said for $TiO_2$-16.6% $SiO_2$–A–72–600 the addition of silica is detrimental to the photocatalysis behavior of titania, while in the case of $TiO_2$-16.6% $SiO_2$–B–72–600 silica can promote the photoactivity due to the efficient generation of Ti–O–Si hetero linkages. This conclusion is supported by the fact depicted in Fig. 1 that the photoactivity of $TiO_2$-16.6% $SiO_2$–A–72–600 is lower than that of $TiO_2$–A–72–600, while $TiO_2$-16.6% $SiO_2$–B–72–600 exhibits better photoactivity than $TiO_2$–B–72–600.

Table 1
The crystalline sizes and adsorption percentage towards the photodegradation of *n*-heptane for the catalysts prepared via different routes and aging time

| Catalysts | Crystalline size (nm) | Adsorption (%) |
|---|---|---|
| $TiO_2$–A–72–600 | 30.3 | 14.7 |
| $TiO_2$–B–72–600 | 39.5 | 8.1 |
| $TiO_2$-16.6% $SiO_2$–A–72–600 | 17.8 | 26.4 |
| $TiO_2$-16.6% $SiO_2$–B–24–600 | 18.6 | 27.1 |
| $TiO_2$-16.6% $SiO_2$–B–72–600 | 15.9 | 34.8 |

As Ti sol and Si sol are mixed, rapid hydrolysis and condensation of Ti-alkoxide leads to the formation of Ti-rich cores and the subsequent development of Si-rich shell [2]. As for route A, at the initial phase of synthesis reaction very dense Si-rich shell is formed on Ti-rich cores and obscures much of their surface sites because of rather high Si/Ti ratio in this period. With the further addition of Ti-alkoxide, the Si/Ti ratio drops down, meaning silica cannot mix with titania uniformly. In this case, some Ti-rich cores are covered by too much silica, while other can only react with a relatively small amount of silica. However, route B can significantly avoid this adverse effects of route A because the simultaneous and slow addition of Si sol and Ti sol can keep the Si/Ti ratio in the reaction solution essentially constant during the whole period of synthesis reaction and thereafter guarantee to form more homogeneous mixed oxide.

Comparing the photocatalysis behaviors of pure $TiO_2$ and $TiO_2$–$SiO_2$ prepared via different routes, we found higher ratio of $OH^-$/Ti in the synthesis solution is beneficial for preparing pure $TiO_2$ with good photoactivity. By contrast, for $TiO_2$–$SiO_2$ adsorption of more identical charges on primary titania particles is detrimental to generate homogeneous mixed oxide, and essentially unchanged Si/Ti ratio in the synthesis solution during the whole synthesis phase may be better. The enhanced homogeneity of mixed oxide more effectively inhibits the growth of crystalline size and promotes the adsorption capability towards *n*-heptane (Table 1).

Fig. 1 also displayed the variation of photoactivity for $TiO_2$–$SiO_2$ aged 24 and 72 h. Evidently, longer aging time favors for obtaining higher photoactivity. Since TBOT is completely hydrolyzed in the initial synthesis phase due to its faster hydrolysis, we infer the better photoactivity owing to longer aging time should be attributed to the enhanced homogeneity of $TiO_2$–$SiO_2$ induced by the full hydrolysis of TEOS.

In order to confirm route B and longer aging time can promote the homogeneity of $TiO_2$–$SiO_2$, the samples were further characterized by FT-IR and SPS, as shown in Figs. 2 and 3. One can see from Fig. 2 that all the samples exhibit the FT-IR bands at 1040 and 931 $cm^{-1}$, which can be assigned to asymmetric $V_{as}$(Si–O–Si) stretching vibration and Ti–O–Si hetero linkages, respectively [9]. It is deserved to note the intensities of 1623 and 466 $cm^{-1}$ bands undergo

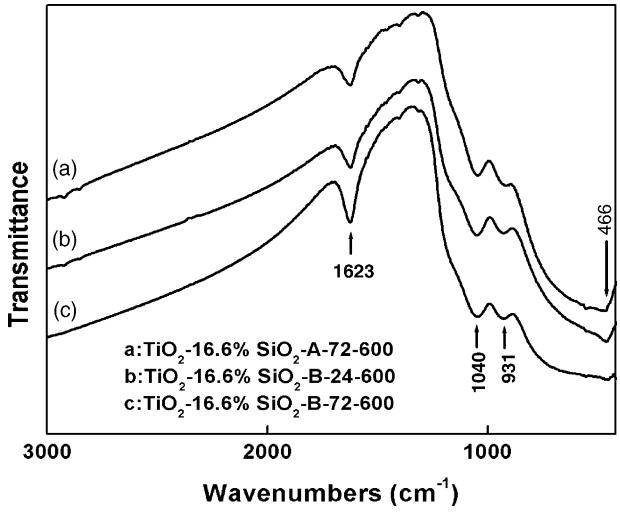


Fig. 2. FT-IR spectra of $TiO_2$-16.6% $SiO_2$ prepared via different synthesis routes and aging time.

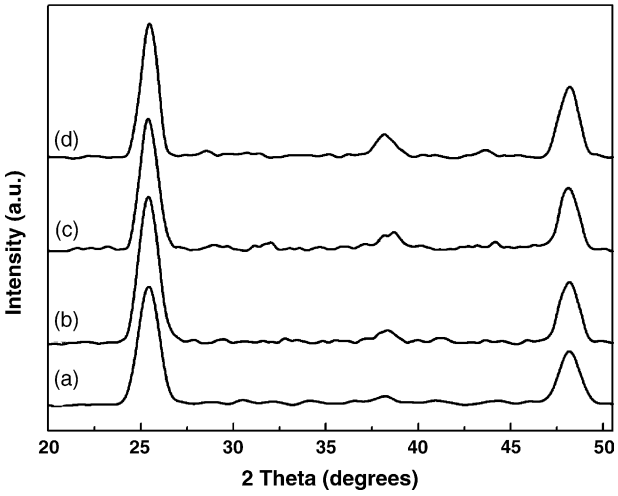


Fig. 4. XRD patterns of $TiO_2$-16.6% $SiO_2$–B–72–600 prepared by using different alcohols as the solvent: (a) methanol; (b) ethanol; (c) propanol; (d) butanol.

some alterations with varying synthesis parameters. Firstly, in $TiO_2$-16.6% $SiO_2$–B–72–600 the decrease of 466 $cm^{-1}$ band that can be ascribed to Si–O–Si bending modes, demonstrates the structure of Si–O–Si is destroyed and more Ti–O–Si hetero linkages are produced as compared with $TiO_2$-16.6% $SiO_2$–A–72–600 and $TiO_2$-16.6% $SiO_2$–B–24–600. Meanwhile, the 1623 $cm^{-1}$ band assigned to the surface hydroxyl groups is much stronger in $TiO_2$-16.6% $SiO_2$–B–72–600, confirming good homogeneity is beneficial for obtaining more surface hydroxyl groups.

Surface photovoltage spectrum (SPS) reflects the separation and recombination of photo-induced electron-hole pairs on the catalyst surface with the aid of illumination [19]. In Fig. 3, due to the presence of more surface hydroxyl groups, $TiO_2$-16.6% $SiO_2$–B–72–600 exhibits remarkably weaker SPS signal than $TiO_2$-16.6% $SiO_2$–A–72–600 and $TiO_2$-16.6% $SiO_2$–B–24–600. Since the intensity of SPS response mainly depends on the net charge on the catalyst

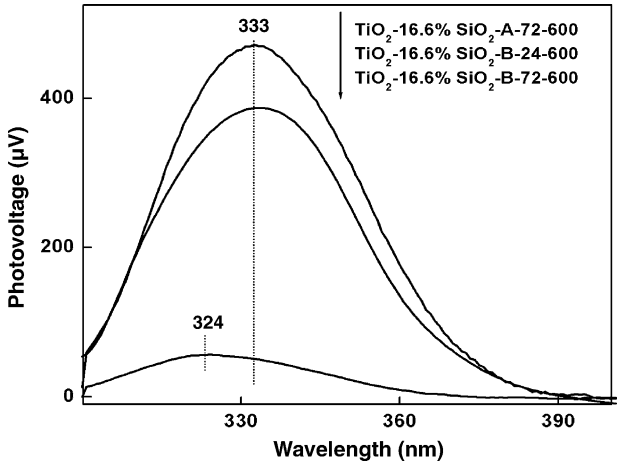


Fig. 3. SPS response signals of $TiO_2$-16.6% $SiO_2$ prepared via different synthesis routes and aging time.

surface, more surface hydroxyl groups can capture so much photo-induced holes ($h^+$) that its SPS signal will be dramatically decreased. Furthermore, compared with $TiO_2$-16.6% $SiO_2$–A–72–600 and $TiO_2$-16.6% $SiO_2$–B–24–600, the SPS peak of $TiO_2$-16.6% $SiO_2$–B–72–600 shifts to lower wavelength, reflecting its band gap is further enlarged because its enhanced homogeneity is more effective in modifying the electronic structure of titania by the generation of more Ti–O–Si hetero linkages that can elevate the conduction band edge and lower the valence band edge. Combining the results of FT-IR and SPS, we conclude the homogeneity of $TiO_2$-16.6% $SiO_2$–B–72–600 is enhanced as compared with $TiO_2$-16.6% $SiO_2$–A–72–600 and $TiO_2$-16.6% $SiO_2$–B–24–600.

### 3.2. Effects of solvent on the photoactivity of $TiO_2$–$SiO_2$

It can be evidently seen from XRD patterns shown in Fig. 4 that the crystallinity of mixed oxide prepared via different alcohols, is increased because the intensity of diffraction peak at 37.8° is increased as the solvent is changed from methanol to butanol. According to the colloidal stability DLVO theory, particles interacting with van der Waals attractive and electrostatic repulsive forces become more stable against aggregation when the surface potential of particles is of sufficient magnitude. The energy barrier ($V_b$), inhibiting the formation of particle aggregation between the particles can be described as follows [20]:

$$V_b = -\frac{Ak\alpha}{12} + 2\pi\varepsilon_0\varepsilon_r\alpha\psi^2$$

where $A$ is effective Hamaker constant, $k$ the Debye-HÜckel constant, $\alpha$ the particle diameter, $\varepsilon_0$ the dielectric of a vacuum, $\varepsilon_r$ the relative dielectric constant of the liquid medium and $\psi$ is the surface potential. From this equation we can see energy barrier ($V_b$) is closely related with the relative dielectric constant of the liquid medium.

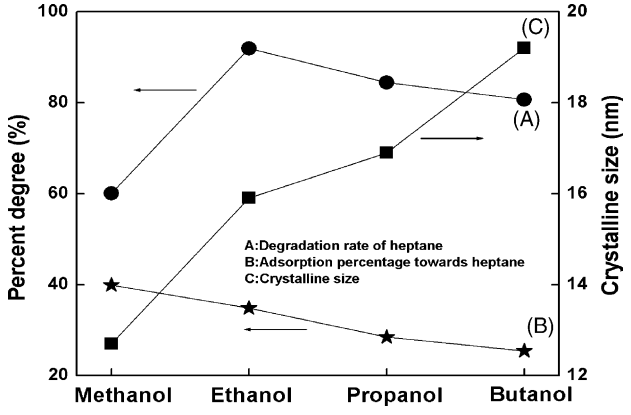


Fig. 5. The variation of photodegradation rate, adsorption percentage and crystalline size for $TiO_2$-16.6% $SiO_2$–B–72–600 with the variation of solvent from methanol to butanol (the photoactivity data referred here were obtained by irradiating the catalysts for 1 h).

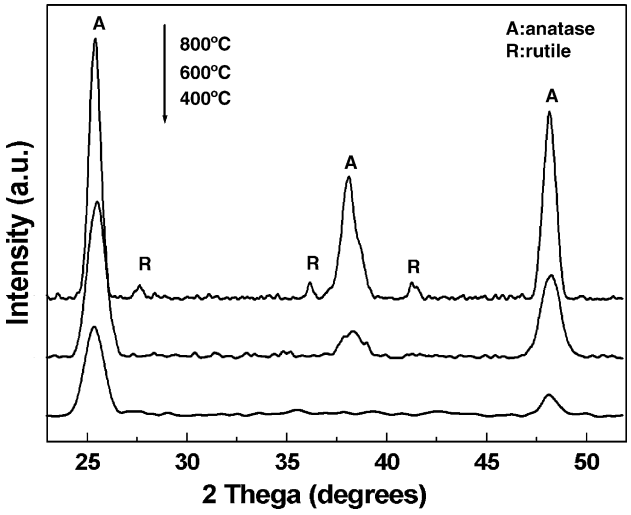


Fig. 6. XRD patterns of $TiO_2$-9.1% $SiO_2$–B–72 calcined at different temperatures.

Since the order of dielectric constant of alcohol used is methanol > ethanol > propanol > butanol, when methanol is used as the solvent the energy barrier ($V_b$) between the primary silica particles is higher and more effective in preventing the collision and aggregation of those particles due to higher dielectric constant of methanol. However, as the solvent is varied from methanol to butanol, the relative dielectric constant is diminished. Thus, the primary silica particles gradually become easy to aggregate together to form bigger particles. We can assume there should have more primary silica particles in the synthesis solution to react with titania as using methanol as the solvent, and consequently inhibit the rapid growth of titania. However, this may exert a negative effect on mixed oxide: its crystallinity will be greatly suppressed. Concerning the mixed oxide prepared by propanol and butanol, the aggregation between the primary silica particles is relative severe, hence, the homogeneity of mixed oxide should be destroyed, justified from its larger crystalline size and lower absorption capability towards *n*-heptane shown in Fig. 5. We also see from Fig. 5 that the photoactivity of mixed oxide via methanol is the lowest because its crystallinity is suppressed. With changing the solvent from methanol to ethanol, the photoactivity reaches the maximum and then drops down as the solvent is further changed from ethanol to propanol or butanol. This decrease in photoactivity should be attributed to the larger crystalline size and lower absorption capability associated with their bad homogeneity. Thus, we can infer the mixed oxide prepared via ethanol should have the best combination of crystalline size, crystallinity, and homogeneity.

### *3.3. Effects of calcination temperature on the structure, surface, and photoactivity properties of $TiO_2$–$SiO_2$*

Fig. 6 exhibited XRD patterns of $TiO_2$-9.1% $SiO_2$–B–72 calcined at 400, 600, and 800 °C. We can observe stronger anatase diffraction peaks at 25.2, 37.8, and 48.0° in $TiO_2$-9.1% $SiO_2$–B–72–600. However, except anatase diffraction peaks $TiO_2$-9.1% $SiO_2$–B–72–800 possesses small rutile diffraction peaks at 27.4, 36.1, and 41.2°, revealing some anatase is transformed to rutile. Furthermore, for $TiO_2$-9.1% $SiO_2$–B–72–400 only two anatase diffraction peaks at 25.2 and 48.0° can be observed, indicating in this sample exists amorphous titania.

The XPS spectra for Si 2p and Ti 2p were shown in Fig. 7. The peak of Si 2p for $TiO_2$-9.1% $SiO_2$–B–72–400 is located around 102.3 eV. With the increase of calcination temperature the peak around 103.6 eV progressively becomes stronger, and meanwhile the peak around 102.3 eV diminishes. This fact demonstrates the chemical environment of silica undergoes a great alteration with increasing the calcination temperature. In the case of $TiO_2$-9.1% $SiO_2$–B–72–400, silica primarily exists in the form of Si–O–Si linkages, while above 600 °C a portion of Si–O–Si linkages will be destroyed, and silica will closely interact with titania to form Ti–O–Si hetero linkages. The fact shown in Fig. 7(b) that the value of Ti $2p_{3/2}$ is gradually increased with the increase of calcination temperature is also an apparent evidence of generating Ti–O–Si hetero linkages above 600 °C. This is because the formation of Ti–O–Si linkages can significantly change the electronic structure of Ti species in $TiO_2$–$SiO_2$, and increase the effective positive charge on the Ti species due to the decrease of the electron density around Ti species resulting from the greater electronegativity of Si via O acting on Ti [2]. Additionally, Fig. 8 exhibited the XPS spectra of O 1s region and its curve-fitting results for $TiO_2$-9.1% $SiO_2$–B–72 calcined at 400 and 600 °C. Interestingly, $TiO_2$-9.1% $SiO_2$–B–72–600 contains Ti–O–Si hetero linkages, while $TiO_2$-9.1% $SiO_2$–B–72–400 does not. The facts shown in Figs. 7 and 8 effectively illustrate: (1) 400 °C is not high enough to produce intimate interaction between titania and silica, thus they mainly exist as two independent components (Ti–O–Ti and Si–O–Si linkages) in $TiO_2$-9.1% $SiO_2$–B–72–400; (2) with increasing the calcination temperature to 600 °C intimate interaction

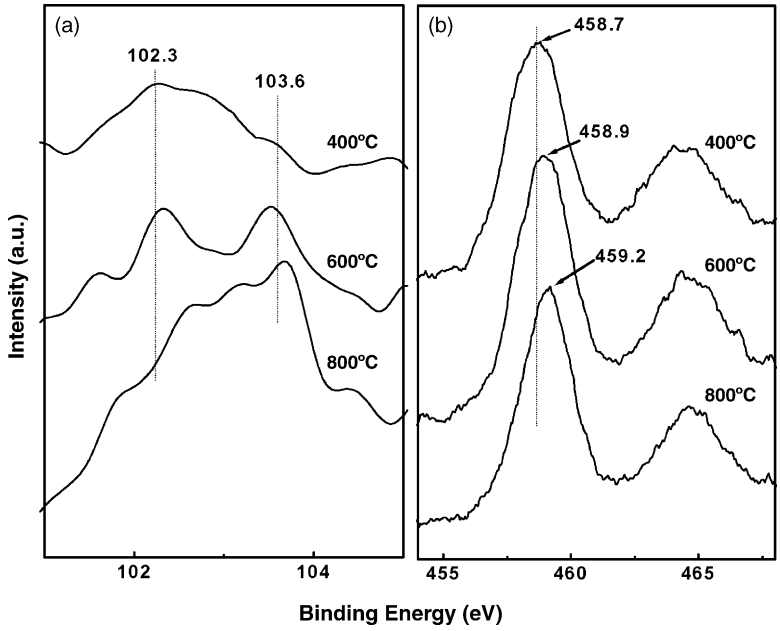


Fig. 7. XPS spectra of Si 2p (a) and Ti 2p (b) for $TiO_2$-9.1% $SiO_2$–B–72 calcined at different temperatures.

between titania and silica (Ti–O–Si hetero linkages) begins to form.

Fig. 9 displayed the photodegradation of *n*-heptane using $TiO_2$-9.1% $SiO_2$–B–72 calcined at different temperatures as the catalysts. It is reasonable that $TiO_2$-9.1% $SiO_2$–B–72–400 possesses the worst photoactivity among three catalysts due to the presence of amorphous titania and no intimate interaction between titania and silica. At 600 °C, the amorphous titania will be transformed to anatase, hinting the bulk defects should be enormously removed. Most importantly, the intimate interaction between titania and silica is formed. The synergism between Ti–O–Si hetero linkages and surface hydroxyl groups can efficiently retard the recombination of photo-induced electron-hole pairs [2]. The formation of Ti–O–Si hetero linkages can enhance the quantum efficiency of mixed oxide, and the oxidizing potential of the photo-induced holes ($h^+$) [1], which is a very important contribution to its enhanced photoactivity. Furthermore, surface hydroxyl groups play a crucial role by accepting photo-induced holes to form OH radicals that can oxidize the species adsorbed on the surface. The significantly decreased photoactivity of $TiO_2$-9.1% $SiO_2$–B–72–800 results from the

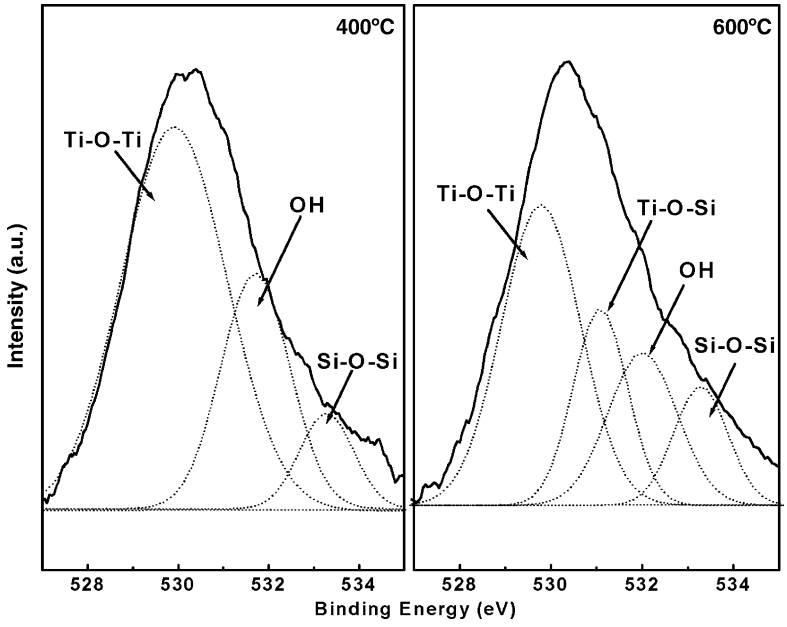


Fig. 8. XPS spectra of O 1s region for $TiO_2$-9.1% $SiO_2$–B–72 calcined at 400 and 600 °C.

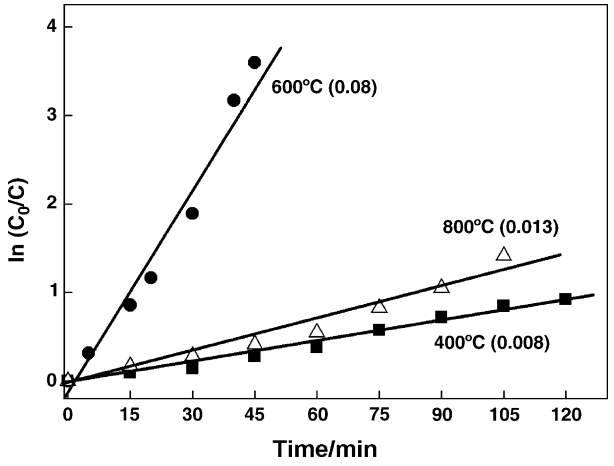


Fig. 9. Photodegradation kinetics of *n*-heptane by $TiO_2$-9.1% $SiO_2$–B–72 calcined at different temperatures, the number in the parenthesis is reaction rate constant.

remarkable removal of surface hydroxyl groups and the transformation of part of anatase titania to rutile. So, the synergism between Ti–O–Si hetero linkages and surface hydroxyl groups is destroyed. Moreover, the absorption capability of rutile titania towards $O_2$, $H_2O$ and reactant molecules as well as the subsequent reactions between these species and photo-induced electron-hole pairs is substantially lower than that of anatase.

## 4. Conclusion

The present work investigated the effects of a series of synthesis parameters, involving synthesis route, aging time and the type of alcohol as well as calcination temperature, on the physico-chemical properties and photoactivity of $TiO_2$–$SiO_2$ prepared by using ammonia–water solution as the hydrolysis catalyst. Based on the experiment results, the following conclusions can be drawn:

(1) Synthesis route has significantly different influences on surface and structure properties as well as photoactivity performance of pure $TiO_2$ and $TiO_2$–$SiO_2$. For pure $TiO_2$, the synthesis route with higher $OH^-$/Ti ratio (route A) will obtain smaller crystalline size and good photoactivity because the aggregation of primary titania particles is inhibited, while for $TiO_2$–$SiO_2$ the synthesis route with lower $OH^-$/Ti ratio and essentially unchanged Si/Ti ratio (route B) is beneficial for obtaining homogeneous mixed oxide with smaller crystalline size, and hence superior photoactivity.

(2) Longer aging time is better for enhancing the homogeneity of mixed oxide in that TEOS can be fully hydrolyzed and generate more Ti–O–Si hetero linkages with titania.

(3) $TiO_2$–$SiO_2$ using ethanol as the solvent has the highest photoactivity among the mixed oxides prepared via different alcohols because of its best combination of crystalline size, crystallinity, and homogeneity.

(4) Upon 600 °C calcination, $TiO_2$–$SiO_2$ possesses pure anatase titania without rutile phase, meaning bulk defects should be greatly removed. Furthermore, the synergism between Ti–O–Si hetero linkages and surface hydroxyl groups is effective in retarding the recombination of photo-induced electron-hole pairs. Therefore, $TiO_2$-9.1% $SiO_2$–B–72–600 has excellent photoactivity. As for $TiO_2$-9.1% $SiO_2$–B–72–400, titania and silica exist as the independent component without intimate interaction. Meanwhile, the existence of amorphous titania is another important contribution to its bad photoactivity. The inferior photoactivity of $TiO_2$-9.1% $SiO_2$–B–72–800 should be assigned to the fact that part of anatase titania is transformed to rutile, and the synergism between Ti–O–Si hetero linkages and surface hydroxyl groups is disrupted.

## Acknowledgment

This work was supported by a grant from the National Natural Science Foundation of China (No. 20277015).

## References

[1] M.R. Hoffmann, S.T. Martin, W. Choi, D.W. Bahnemann, Chem. Rev. 95 (1995) 69.
[2] X. Gao, I.E. Wachs, Catal. Today 51 (1999) 233.
[3] Y. Xu, C.H. Langford, J. Phys. Chem. B 101 (1997) 3115.
[4] J.C. Yu, J. Lin, R.W.M. Kwok, J. Phys. Chem. B 102 (1998) 5094.
[5] J.B. Miller, E.I. Ko, Catal. Today 35 (1997) 269.
[6] J.B. Miller, S.T. Johnston, E.I. Ko, J. Catal. 150 (1994) 311.
[7] R. Hutter, T. Mallat, A. Baiker, J. Catal. 153 (1995) 177.
[8] Y. Xu, W. Zheng, W. Liu, J. Photochem. Photobiol. A: Chem. 122 (1999) 57.
[9] D.C.M. Dutoit, M. Schneider, A. Baiker, J. Catal. 153 (1995) 165.
[10] D.C.M. Dutoit, M. Schneider, R. Hutter, A. Baiker, J. Catal. 161 (1996) 651.
[11] D.C.M. Dutoit, U. Gobel, M. Schneider, A. Baiker, J. Catal. 164 (1996) 433.
[12] C. Anderson, A.J. Bard, J. Phys. Chem. B 101 (1997) 2611.
[13] K.Y. Jung, S.B. Park, Appl. Catal. B 25 (2000) 249.
[14] X.Z. Fu, L.A. Clark, Q. Yang, M.A. Anderson, Environ. Sci. Technol. 30 (1996) 647.
[15] P. Cheng, M.P. Zheng, Y.P. Jin, Q. Huang, M.Y. Gu, Mater. Lett. 57 (2003) 2989.
[16] J. Yu, J.C. Yu, M.K.-P. Leung, W. Ho, B. Cheng, X. Zhao, J. Zhao, J. Catal. 217 (2003) 69.
[17] W. Stober, A.J. Fink, E. Bohn, J. Colloid Interf. Sci. 26 (1968) 62.
[18] L. Zhao, J. Yu, P. Cheng, J. Zhao, Acta Chim. Sinica 61 (2003) 562.
[19] L.Q. Jing, X.J. Sun, W.M. Cai, Sol. Energ. Mater. Sol. Cells 79 (2003) 133.
[20] H.Y. Park, Y.T. Moon, D.Y. Kim, C.H. Kim, J. Am. Ceram. Soc. 79 (1996) 2727.